

# Lithium and Sodium Ion Binding Energies of *N*-Acetyl and *N*-Glycyl Amino Acids

Wan Yong Feng,<sup>†</sup> Scott Gronert,<sup>\*,†</sup> and Carlito B. Lebrilla<sup>‡</sup>

Contribution from the Department of Chemistry and Biochemistry, San Francisco State University, San Francisco, California 94132, and Department of Chemistry, University of California, Davis, California 95616

Received August 31, 1998

**Abstract:** Using a quadrupole ion-trap mass spectrometer with an electrospray ionization source, the Cooks kinetic method has been used to measure the lithium and sodium ion binding energies of the *N*-acetyl and *N*-glycyl derivatives of a series of 14 amino acids. For comparison, the gas-phase basicities of the amino acid derivatives were also determined by the kinetic method. The lithium binding free energies range from 47.2 to 56.4 kcal/mol, and the sodium affinities from 30.8 to 41.2 kcal/mol. Comparisons between basicities and metal ion binding energies indicate that the presence of a coordinating group (e.g.,  $-\text{OH}$ ,  $-\text{CO}_2\text{H}$ , etc.) in the amino acid side chain can significantly increase the lithium and sodium binding energies. Dynamics calculations (CHARMm) confirm that side-chain coordination is a common stabilizing effect in the metalated systems. A good correlation, with a slope near unity, is found between the metal ion binding energies of the *N*-acetyl and *N*-glycyl derivatives. This indicates that the two groups of compounds are adopting similar coordination schemes and strongly suggests that zwitterionic forms of the peptide derivatives are not important.

## Introduction

The development of electrospray ionization (ESI)<sup>1,2</sup> and matrix-assisted laser desorption ionization (MALDI)<sup>3</sup> techniques has greatly enhanced the ability of chemists to study large molecules in the gas phase and opened the door to important new applications in chemical analysis. One area that has been the focus of intense interest is the use of mass spectrometry in the identification and sequencing of peptides.<sup>4–7</sup> Efforts in this area have involved singly and multiply protonated or deprotonated peptides as well as metal complexes of neutral or charged peptides.<sup>8–15</sup> From these studies, it is apparent that the charge site can play a critical role in determining location of bond cleavages during fragmentation pathways.<sup>16,17</sup> Although for the simplest peptides the location of the charge carrier (metal ion)

can be predicted with reasonable certainty, this is not the case for larger peptides with many side chains containing a range of functional groups.<sup>18</sup> As a result, predicting fragmentation patterns in these peptides is, to some extent, limited by our ability to predict the location of the metal ion.

The site of metalation is controlled by several factors. The most important factor is the inherent Lewis basicity of the coordinating functional group. For lithium, work in several groups has led to the determination of ion affinities for many ligands including all of the functional groups typically found in peptides.<sup>19–25</sup> For other metals, much less information is available in the literature.<sup>26,27</sup> However, values have been reported for the  $\text{Na}^+$  and  $\text{Cu}^+$  affinities of the common amino acids.<sup>28,29</sup> In addition, Wesdemiotis and Kebarle have investigated the sodium affinities of some dipeptides.<sup>27,30</sup> Along with the basicity of the functional group, one must also consider the

<sup>†</sup> San Francisco State University.

<sup>‡</sup> University of California, Davis.

(1) Fenn, J. B.; Mann, M.; Meng, C. K.; Wong, S. F.; Whitehouse, C. M. *Science* **1985**, *246*, 64.

(2) Yamashita, M.; Fenn, J. B. *J. Phys. Chem.* **1984**, *88*, 4451.

(3) Karas, M.; Hillenkamp, F. *Anal. Chem.* **1988**, *60*, 2299.

(4) Biemann, K. *Biomed. Environ. Mass Spectrom.* **1988**, *16*, 99.

(5) Gross, M. L. *Acc. Chem. Res.* **1994**, *27*, 361.

(6) Patterson, S. D. *Anal. Biochem.* **1994**, *221*, 1.

(7) Chait, B. T.; Kent, S. B. H. *Science* **1992**, *257*, 1885.

(8) Leary, J. A.; Williams, T. D.; Bott, G. *Rapid Commun. Mass Spectrom.* **1989**, *3*, 192.

(9) Hopper, S.; Johnson, R. S.; Vath, J. E. *J. Biol. Chem.* **1989**, *264*, 20438.

(10) Hunt, D. F.; Yates, J. R., III; Shabanowitz, J.; Bruns, M. E.; Bruns, D. E. *J. Biol. Chem.* **1989**, *264*, 6580.

(11) Yates, J. R., III; Eng, J. K.; McCormack, A. L.; Schieltz, D. *Anal. Chem.* **1995**, *67*, 1426.

(12) Castoro, J. A.; Wilkins, C. L.; Woods, A. S.; Cotter, R. J. *J. Mass Spectrom.* **1995**, *30*, 94.

(13) Doroshenko, V. M.; Cotter, R. J. *Anal. Chem.* **1995**, *67*, 2180.

(14) Teesch, L. M.; Adams, J. *J. Am. Chem. Soc.* **1991**, *113*, 812.

(15) Teesch, L. M.; Adams, J. *J. Am. Chem. Soc.* **1991**, *113*, 3668.

(16) Leary, J. A.; Zhou, Z.; Ogden, S. A.; Williams, T. D. *J. Am. Soc. Mass Spectrom.* **1990**, *1*, 473.

(17) Tang, X. J.; Thibault, P.; Boyd, R. K. *Org. Mass Spectrom.* **1993**, *28*, 1047.

(18) Kenny, P. T. M.; Nomoto, K.; Orlando, R. *Rapid Commun. Mass Spectrom.* **1997**, *11*, 224.

(19) Staley, R. H.; Beauchamp, J. L. *J. Am. Chem. Soc.* **1975**, *97*, 5920.

(20) Woodin, R. L.; Beauchamp, J. L. *J. Am. Chem. Soc.* **1978**, *100*, 501.

(21) Taft, R. W.; Anvia, F.; Gal, J.-F.; Walsh, S.; Capon, M.; Holmes, M. V. H., K.; Oloumi, G.; Vasanwala, R.; Yazdani, S. *Pure Appl. Chem.* **1990**, *62*, 17.

(22) Rodgers, M. T.; Armentrout, P. B. *J. Phys. Chem. A* **1997**, *101*, 2614.

(23) Ray, D.; Feller, D.; Armentrout, P. B. *J. Phys. Chem.* **1996**, *100*, 16116.

(24) More, M. B.; Ray, D.; Armentrout, P. B. *J. Phys. Chem. A* **1997**, *101*, 831.

(25) More, M. B.; Ray, D.; Armentrout, P. B. *J. Phys. Chem. A* **1997**, *101*, 4254.

(26) Davidson, W. R.; Kebarle, P. *J. Am. Chem. Soc.* **1976**, *98*, 6133.

(27) Klassen, J. S.; Anderson, S. G.; Blades, A. T.; Kebarle, P. *J. Phys. Chem.* **1996**, *100*, 14218.

(28) Bojessen, G.; Breindahl, T. J.; Anderson, U. N. *Org. Mass Spectrom.* **1993**, *28*, 1448.

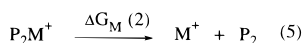
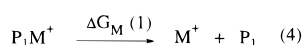
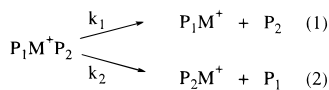
(29) Cerda, B. A.; Wesdemiotis, C. *J. Am. Chem. Soc.* **1996**, *117*, 9734.

(30) Cerda, B. A.; Hoyau, S.; Ohanessian, G.; Wesdemiotis, C. *J. Am. Chem. Soc.* **1998**, *120*, 2437.

possibility of multidentate coordination to several functional groups in the peptide. For example, Lebrilla and others have investigated multidentate coordination in protonated polyglycines.<sup>31–35</sup>

In the present study, we examine the ion affinities of a series of *N*-acetyl and *N*-glycyl amino acids using an ion-trap mass spectrometer with an electrospray ionization source. These compounds provide simple models of amino acids in a peptide chain. The *N*-acetyl series allows us to investigate the cooperative binding of the metal ion to the amide (peptide bond) and the side-chain functional group. In the *N*-glycyl series, the additional *N*-terminal amino group provides another strong Lewis base (metal binding site) and the possibility of a higher coordination state for the metal. Fourteen amino acids have been considered. The most basic amino acids (Arg, His, and Lys) were excluded because their binding energies are exceptionally high and are not easily linked via kinetic measurements to the other derivatives.<sup>36</sup> For each of the compounds, we have determined the Li<sup>+</sup> and Na<sup>+</sup> binding energies. In addition, their gas-phase basicities were measured.

In terms of an experimental approach, there are significant limitations on measuring the metal binding energies of gaseous peptides. First, the low volatility of the peptides does not allow for methods based on establishing a gas phase equilibrium. Second, the complexity of the substrates would make the dynamics analysis of dissociation threshold measurements extremely difficult. Under these circumstances, the Cooks kinetic method<sup>37,38</sup> becomes a logical choice. It has already been used to measure the ion affinities (proton and metal) of a wide range of species that are not amenable to traditional methods (i.e., equilibrium or dissociation threshold). For example, the kinetic method recently has been applied to the metal affinities of amino acids and small peptides.<sup>28–30</sup> This approach has proven to be accurate and reliable when it has been used to compare species that are closely related. The application of the Cooks kinetic approach to metal ion binding energies involves the formation of a ternary complex (P<sub>1</sub>M<sup>+</sup>P<sub>2</sub>) between the cation and the two peptides whose binding energies are to be compared (P<sub>1</sub> and P<sub>2</sub>). Collision-induced dissociation (CID) of the complex leads to the loss of one peptide. Since either peptide can be lost, the product ratio gives a measure of the relative peptide binding energy. If one assumes that the stabilities of the dissociation transition states are directly related to the stabilities of the dissociation products (i.e., “late” transition state), then the ratio of dissociation rates ( $k_1/k_2$ ) is approximately equivalent to the equilibrium constant of eq 3. The ratio of  $k_1/k_2$  is equal to the ratio of ion intensities,  $I(P_1M^+)/I(P_2M^+)$  because the dissociation is irreversible under the reaction conditions.



(31) Wu, J.; Lebrilla, C. *J. Am. Chem. Soc.* **1993**, *115*, 3270.

(32) Wu, J.; Lebrilla, C. *J. Am. Soc. Mass Spectrom.* **1995**, *6*, 91.

(33) Wu, Z.; Fenselau, C. *J. Am. Soc. Mass Spectrom.* **1992**, *3*, 863.

(34) Cheng, X.; Wu, Z.; Fenselau, C. *J. Am. Chem. Soc.* **1993**, *115*, 4844.

(35) Zhang, K.; Zimmerman, D. M.; Chung-Phillips, A.; Cassady, C. J. *J. Am. Chem. Soc.* **1993**, *115*, 10812.

(36) Studies are underway on these species and will be reported soon.

The observed intensities can be converted to thermodynamic values in the following way:

$$I(P_1M^+)/I(P_2M^+) = k_1/k_2 \approx K \quad (6)$$

$$-RT_{\text{eff}} \ln K = \Delta G_M(1) - \Delta G_M(2) \quad (7)$$

where  $\Delta G_M(1)$  and  $\Delta G_M(2)$  are the binding free energies for P<sub>1</sub> and P<sub>2</sub>, respectively, and  $T_{\text{eff}}$  is the effective temperature of the system during the dissociation process. The assumption inherent in eq 6 is that the reverse activation barriers of the reactions in eqs 1 and 2 are equal. In ion traps,  $T_{\text{eff}}$  is usually slightly above the temperature of the bath gas.<sup>39,40</sup> Because we are unable to measure binding constants as a function of temperature, it is not possible to extract the enthalpy and entropy of binding from the data. Consequently the values are reported as free energies.<sup>41</sup>

The Cooks method gives the differences in binding energies between pairs of peptides. By examining numerous peptide combinations, ladders of relative binding energies were generated. By including species of known binding energy, the relative scales were converted to absolute values.

## Methods

All measurements were made with a Finnigan LCQ ion-trap mass spectrometer operating with a background helium pressure of  $1.75 \times 10^{-3}$  Torr. All reagents were obtained from commercial sources and were used without further purification. Typical operating conditions involve an ESI needle voltage of about 4 kV, a solution flow rate of 3–8  $\mu\text{L}/\text{min}$ , and a heated capillary temperature of about 150 °C. The samples were prepared as methanol solutions ( $10^{-5}$ – $10^{-3}$  M), and the appropriate alkali metal halide was added to the solution of the two ligands. The dimer ions generated by ESI were isolated using the LCQ advanced scan software and activated for 3–10 ms with an activation voltage of  $\sim 0.5$  V. Each measurement of the product ion intensity ratio usually was an average of 10–50 scans and repeated six times. About 1000 scans were averaged for product ions with low intensities. Experimental uncertainty in the abundance ratios of the fragment ions was estimated as  $\pm 12\%$ . This leads to an uncertainty of  $\pm 5\%$  in the natural log of the ratio. Given the uncertainties in the ion affinities of standard reference bases as well as those in the kinetic measurements, the present values are assigned absolute uncertainties of  $\pm 2.5$  kcal/mol; however, the relative errors are expected to be much smaller ( $\pm 1$  kcal/mol).

In most cases, the relative ion binding energies were determined on the basis of measurements with more than one combination of ligands. The binding energy ladder was then determined using a least-squares approach. In several cases, the dissociation produces a minor amount other ligand fragmentation products (i.e., loss of H<sub>2</sub>O, CO<sub>2</sub>, etc.) In

(37) Cooks, R. G.; Patrick, J. S.; Kotiaho, T.; McLuckey, S. A. *Mass Spectrom. Rev.* **1994**, *13*, 287.

(38) McLuckey, S. A.; Cameron, D.; Cooks, R. G. *J. Am. Chem. Soc.* **1981**, *103*, 1313.

(39) Brodbelt-Lustig, J. S.; Cooks, R. G. *Talanta* **1989**, *36*, 255.

(40) Feng, W. Y.; Gronert, S. *J. Phys. Chem. A.*, submitted.

(41) The free energies reported in this paper are referenced to 300 K. Some workers have used  $T_{\text{eff}}$  as a real thermodynamic quantity and assumed that their CID studies give equilibrium constants ( $K$  in eq 3) at  $T_{\text{eff}}$ . This may be true in some cases, but it is unlikely that the CID energy is always randomized throughout the complex before dissociation. Moreover, this does not take into account that  $T_{\text{eff}}$  also provides a correction for “early” dissociation transition states (i.e., situations where the difference in product channel energies is not fully realized at the transition state for dissociation). However, it is reasonably safe to assume that the kinetic method is giving a measure of the equilibrium constant at a temperature somewhere between 300 K and  $T_{\text{eff}}$ . Given that  $T_{\text{eff}}$  is close to 300 K in our experiments, the most logical choice is to report the data as free energies at 300 K. This allows for the most straightforward comparisons with data in the literature. The maximum error introduced by this choice is small. Even with a large entropy difference in eq 3 (10 eu), the difference in relative free energies at 300 and 350 K is only 0.5 kcal/mol.

**Table 1.** Ion Binding Energies of *N*-Glycylglycine (GG) and *N*-Acetylglycine (NAG) Measured by the Kinetic Method

base	ion-bound dimers <sup>a</sup>	ln( <i>k</i> <sub>2</sub> / <i>k</i> <sub>1</sub> )	ion binding energy (kcal/mol) <sup>b</sup>
GG	GG H <sup>+</sup> - <i>c</i> -C <sub>5</sub> H <sub>5</sub> N	4.75	GB = 211.3
	GG H <sup>+</sup> CH <sub>3</sub> CONMe <sub>2</sub>	-1.52	
	GG H <sup>+</sup> <i>n</i> -C <sub>3</sub> H <sub>7</sub> NH <sub>2</sub>	-0.67	
NAG	C <sub>6</sub> H <sub>5</sub> NH <sub>2</sub> H <sup>+</sup> NAG	4.57	GB = 205.2
	Gly H <sup>+</sup> NAG	0.78	
GG	GC Li <sup>+</sup> GG	-1.05	Δ <i>G</i> <sub>Li</sub> = 49.4
	Leu Li <sup>+</sup> GC	5.63	
	CH <sub>3</sub> CONMe <sub>2</sub> Li <sup>+</sup> Leu	2.14	
NAG	NAC Li <sup>+</sup> NAG	-1.27	Δ <i>G</i> <sub>Li</sub> = 47.2
	GG Li <sup>+</sup> NAC	-1.94	
GG	GC Na <sup>+</sup> GG	0.11	Δ <i>G</i> <sub>Na</sub> = 34.2
	NAL Na <sup>+</sup> GC	0.46	
	Leu Na <sup>+</sup> NAL	2.73	
	Ala Na <sup>+</sup> Leu	2.01	
	CH <sub>3</sub> CONMe <sub>2</sub> Na <sup>+</sup> Ala	0.36	
NAG	NAL Na <sup>+</sup> NAG	-4.83	Δ <i>G</i> <sub>Na</sub> = 30.8

<sup>a</sup> The following abbreviations are used: GG = glycylglycine, NAG = *N*-acetylglycine, GC = glycylcysteine, Gly = glycine, Leu = leucine, NAC = *N*-acetylcysteine, Ala = alanine, and NAL = *N*-acetylleucine.

<sup>b</sup> GB of standards are *c*-C<sub>5</sub>H<sub>5</sub>N = 214.7 kcal/mol, *s*-C<sub>4</sub>H<sub>9</sub>NH<sub>2</sub> = 214.1 kcal/mol, C<sub>6</sub>H<sub>5</sub>NH<sub>2</sub> = 203.3 kcal/mol, CH<sub>3</sub>CONMe<sub>2</sub> = 209.6 kcal/mol, *n*-C<sub>3</sub>H<sub>7</sub>NH<sub>2</sub> = 211.3 kcal/mol, and Gly = 203.7 kcal/mol.<sup>44</sup> Standard values for metal ion binding energies are Δ*G*<sub>Li</sub> (CH<sub>3</sub>CONMe<sub>2</sub>) = 44.7 kcal/mol and Δ*G*<sub>Na</sub> (CH<sub>3</sub>CONMe<sub>2</sub>) = 30.3 kcal/mol. The lithium value originates from Taft's<sup>21,40</sup> study, but contains a correction for a systematic error identified by Rodgers and Armentrout.<sup>22</sup> The sodium value is derived from Kebarle's work.<sup>27</sup>

addition, reactions with residual ESI solvent (ligand switching) were also observed. These reactions do not affect the ratio measurement and can be minimized by adjusting ESI conditions and reducing the activation time.

Dynamics calculations were completed on an SGI octane with the CHARMM force-field implemented in the Quanta computational modeling package.<sup>42</sup> Standard parameters and partial charges were used for the dipeptide derivatives. In some cases the sum of atomic charges differed slightly from zero (±0.1) and the excess charge was smoothed over the nonpolar carbons. Since the goal of the modeling was to identify coordination motifs rather than quantify binding energies, this approximation will have little effect on the conclusions. Simulations were completed at a number of temperatures (300 to 1200 K) and monitored for 10 to 250 ps with a step size of 0.001 ps. During the simulations, structures were stored at intervals from 0.01 to 0.1 ps. Low-energy structures from the simulations were extracted and submitted to full optimization with the CHARMM force-field. A variety of other structures representing important coordination schemes were also extracted and minimized. Finally, the stored structures (1000–3000 per simulation) were used to calculate average molecular geometries.

## Results and Discussion

**Anchor Points for the Scales.** For each of the ion binding energy scales, we have used the simplest representative (i.e. *N*-acetylglycine and glycylglycine) as the anchor point for assigning absolute values. The Δ*G*<sub>M</sub>'s of these peptides were determined with the Cooks method using compounds of known binding energy as references. In Table 1, these studies are summarized. In some cases, several compounds were needed to bridge the gap between the peptide and the reference compound of known binding energy. For example, the lithium binding energy of glycylglycine was linked to dimethylacetamide by measurements involving lysine and glycylcysteine. When possible, redundant determinations were made (bridging the gap with more than one set of intermediates). To convert the measured intensity ratios to binding energy differences, a

value for *T*<sub>eff</sub> is needed. From other studies in our lab, we have estimated values of *T*<sub>eff</sub> for the dissociation of proton- and metal-bound dimers (325 and 350 K, respectively).<sup>40,43</sup> These values are consistent with the value that Brodbelt and Cooks<sup>39</sup> measured in their ion trap for the dissociation of proton bound pyridine dimers. Errors associated with these choices for *T*<sub>eff</sub> are expected to be fairly minor because experience with helium-damped ion traps indicates that *T*<sub>eff</sub> values are usually limited to a fairly narrow range above the temperature of the bath gas. This is in contrast to high-energy CID instruments where *T*<sub>eff</sub> can vary over an exceptionally wide range.<sup>29,30</sup> Finally, the validity of our choice was independently tested for the protonated system (see below).

The gas-phase basicity of glycylglycine has been measured in the past, and our value is in good agreement with the value in Hunter and Lias's compilation<sup>44</sup> (GB = 211 kcal/mol) as well as the values in Harrison's recent review.<sup>45,46</sup> As expected, the gas phase basicity of *N*-acetylglycine is much lower than that of glycylglycine because the highly basic N terminus is missing. Protonation at the amide is expected in *N*-acetylglycine, and the gas-phase basicity is very similar to that of *N*-methylacetamide (205 kcal/mol).<sup>44</sup> In the lithium systems, the ion binding energy of glycylglycine is again greater than that of *N*-acetylglycine; however, both compounds have much higher ion binding energies than monofunctional analogues. For example, the lithium binding energy of glycylglycine is 5 kcal/mol greater than dimethylacetamide and ~10 kcal/mol greater than primary amines. Clearly, the larger size of the cation allows the lithium systems to more effectively engage in multidentate coordination than the protonated systems. In addition, there is only a small difference between the lithium binding energies of the *N*-acetyl and glycyl amino acids. This is not surprising because amides have higher lithium binding energies than amines,<sup>21,40</sup> and therefore the presence of the N-terminal amino group is less important than in the protonated systems (amines have higher proton binding energies than amides). The sodium systems also appear to benefit from multidentate coordination, and the peptides have higher ion binding energies than monofunctional analogues. The sodium binding energy of glycylglycine can be compared with Wesdemiotis and co-workers' recent measurement.<sup>30</sup> Using the Cooks kinetic method with a series of nucleotide bases as standards, they obtained a sodium affinity of 42.3 kcal/mol. Using their estimate of Δ*S*<sup>o</sup>, this can be converted to Δ*G*<sub>Na</sub>(300 K) = 34.0 kcal/mol. This is in very good agreement with our sodium binding energy (34.2 kcal/mol).

**Gas-Phase Basicities.** In Table 2, the gas phase basicities (GB) of the *N*-acetyl and *N*-glycyl amino acids are listed along with values for the gas phase basicities of the bare amino acids. A few trends are apparent in the data. First, the great majority of the glycylylated amino acids are considerably more basic (~5 kcal/mol) than the amino acids. Undoubtedly this is because the extra residue provides an amide functional group as an additional site for hydrogen bonding (or protonation). The

(43) The effective temperature for the proton-bound systems was derived from several sets of experiments involving compounds of known gas-phase basicity. These included kinetic measurements with simple alkylamines as well as amino acids and polyamines: Feng, W. Y. and Gronert, S., unpublished results.

(44) Hunter, E. F.; Lias, S. G. In *NIST Standard Reference Database Number 69*; Mallard, W. G., Linstrom, P. J., Eds.; National Institute of Standards and Technology (<http://webbook.nist.gov>): Gaithersburg, MD, June 1998.

(45) Harrison, A. G. *Mass Spectrom. Rev.* **1997**, *16*, 201.

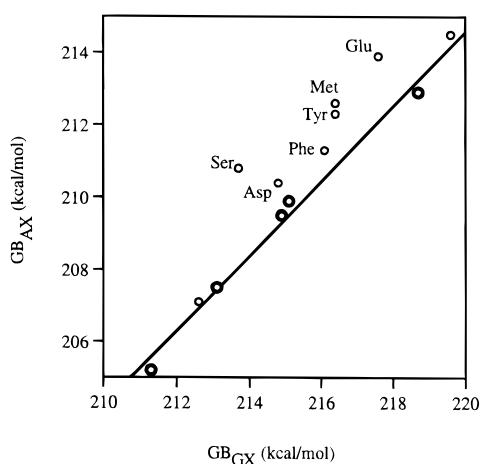
(46) It should be noted that in the Harrison review, the value attributed to Wu and Lebrilla (ref 31) for glycylglycine is too low. Using accepted values for the bracketing reagents, it should be 209.5 kcal/mol.

(42) Quanta: 97.0711: Molecular Simulations, Inc., Waltham, MA, 1998.

**Table 2.** Gas Phase Basicities of Dipeptides and Amino Acids

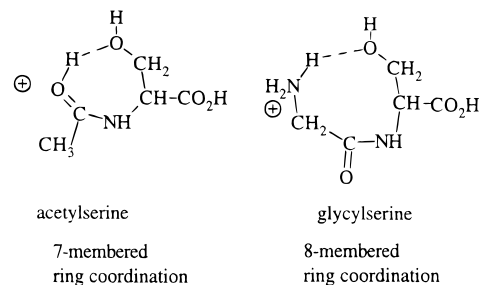
X	GB (kcal/mol)		X <sup>a</sup>
	<i>N</i> -Gly-X	<i>N</i> -acetyl-X	
Trp	219.6	214.5	219.0
Pro	218.7	212.9	211.8
Glu	217.6	213.9	210.1
Tyr	216.4	212.3	213.2
Met	216.4	212.6	215.5
Phe	216.1	211.3	212.5
Leu	215.1	209.9	210.5
Thr	215.0	<i>b</i>	212.4
Val	214.9	209.5	209.5
Asp	214.8	210.4	209.0
Ser	213.7	210.8	210.5
Ala	213.1	207.5	207.4
Cys	212.6	207.1	207.8
Gly	211.3	205.2	203.7

<sup>a</sup> Reference 44. <sup>b</sup> *N*-acetyl threonine was not included in the study.

**Figure 1.** Plot of the gas-phase basicity of the acetylated amino acids ( $GB_{AX}$ ) vs the glycylylated amino acids ( $GB_{GX}$ ).

difference is the greatest for the amino acids that do not have basic functional groups in their side chains (e.g., Gly, Ala, etc.). In contrast, the *N*-acetyl amino acids have gas phase basicities that generally are fairly similar to those of the bare amino acids. Although the *N*-acetylation converts the amine to a somewhat less basic functional group (amide), protonation of the amide allows for more effective hydrogen bonding to the carbonyl of the carboxyl group. As a result, the basicities are reasonably close. Careful analysis of the data indicates that the acetylated amino acids rely more heavily on the side chain for stabilization than the glycylylated derivatives. This can be seen in a plot of acetylated amino acid basicity vs glycylylated amino acid basicity (Figure 1). There is considerable scatter, but a good correlation is found for the derivatives with simple alkyl side chains (Gly, Ala, Val, Leu, Pro). These are marked with heavy circles in the plot and the correlation line is also shown. The slope is near unity (1.03), indicating that changes in alkyl side chains have almost an equal effect on the basicity of the acetyl and glycylyl amino acids. However, many points lie above the line, indicating that these side chains have a greater effect on the basicity of the acetyl derivative than that of the glycylyl derivative. Most notable are Ser and Glu which are several kcal/mol above the correlation line. There are two reasonable explanations for this effect, and both probably play a role. First, since protonation of an amide is less exothermic than protonation of an amine, the acetyl derivatives gain more by an additional coordination site (or polarizable group) in the side chain. Second, protonation

of the amide may place the proton in a better location for forming an internal hydrogen bond with the side chain. For example, hydrogen bonding schemes for serine are shown below.



In the acetyl derivative, a seven-membered ring is required for the internal hydrogen bond, whereas the glycylyl derivative requires an eight-membered ring. This latter point was explored with molecular dynamics. Using the CHARMM force field, the structure of the ammonium ion of glycylylserine (protonation at the N terminus) was monitored in a series of simulations at various temperatures. The dynamics indicate that serine's hydroxyl group has virtually no interaction with the charge site, and minimization of structures with a hydrogen bond between the ammonium ion and the serine hydroxyl oxygen led to relatively unstable conformations. The most common interaction in the simulation is a hydrogen bond between the ammonium and the carbonyl of the C terminus. For acetylserine, the protonated carbonyl oxygen was modeled by a modified imine group. To yield the proper charge, the ab initio (HF/6-31+G\*) charge distribution of carbonyl protonated  $CH_3C(O)NHCH_3$  was applied to the atoms in the model. Dynamics simulations for this system exhibited extensive interaction between the charge center and the serine hydroxyl. In fact, minimization of the low-energy structures from the simulations suggest that a structure with a hydrogen bond between the protonation site and the hydroxyl oxygen represents the global minimum. This result is relatively insensitive to modifications to the charges used in the model. Although not conclusive, the modeling suggests that the side chain can play an important role in stabilizing the protonated acetyl derivatives but is less effective with the glycylyl derivatives. This is certainly consistent with the results in Figure 1.

For some of the dipeptides, the gas-phase basicities have been measured in the past. Because different studies have used different basicity scales for assigning values, it is best to make comparisons in terms of relative values. Most of the work in this area has been completed by the Cassidy group using the bracketing technique.<sup>47-49</sup> For the *N*-glycylylated derivatives of glycine, alanine, serine, and proline, they obtain relative GBs of 0.0, 1.3, 1.3, and 6.8 kcal/mol, respectively. For the same series, we obtain 0.0, 1.8, 2.4, and 7.4 kcal/mol, respectively. The agreement in the relative values is very good, given the inherent uncertainties in the methods; however, our absolute GB values are larger by about 1.5 kcal/mol.<sup>50</sup>

Finally, if there were a serious error in our assignment of  $T_{eff}$ , it would be most apparent at the top of the ladders because

(47) Ewing, N. P.; Zhang, X.; Cassidy, C. J. *J. Mass Spectrom.* **1996**, *31*, 1345.

(48) McKiernan, J. W.; Beltrame, C. E. A.; Cassidy, C. J. *J. Am. Soc. Mass Spectrom.* **1994**, *5*, 718.

(49) Cassidy, C. J.; Carr, S. R.; Zhang, Z.; Chung-Phillips, A. *J. Org. Chem.* **1995**, *60*, 1704.

(50) This conclusion comes from reevaluating Cassidy's bracketing for Gly-Gly using Hunter and Lias's GB values for the standard reference bases.

**Table 3.** Lithium Binding Energies of Dipeptides

X	$\Delta G_{Li}$ (kcal/mol)	
	<i>N</i> -Gly-X	<i>N</i> -acetyl-X
Trp	56.4	54.0
Pro	53.0	51.3
Glu	56.9	54.7
Tyr	53.4	51.3
Met	52.8	51.0
Phe	53.0	51.1
Leu	51.5	50.0
Thr	55.8	<i>a</i>
Val	51.1	49.5
Asp	54.9	52.3
Ser	54.1	51.5
Ala	50.3	48.5
Cys	50.1	48.1
Gly	49.4	47.2

<sup>a</sup> *N*-acetyl threonine was not included in the study.

these compounds have the largest  $\ln k_1/k_2$  values (relative to the anchor points) and the deviation in GB would be most pronounced ( $GB = RT_{eff} \ln k_1/k_2 + GB_{anchor}$ ). To confirm the values at the top of the scales, the gas-phase basicities of glycytryptophan, glycyproline, and *N*-acetyltryptophan were measured in kinetic method experiments against a series of amines with known gas-phase basicities.<sup>44,51</sup> The GB values from these experiments (220.4, 219.1, and 214.1 kcal/mol, respectively) are in reasonable accord with those from the ladders (Table 2). The average deviation (0.3 kcal/mol) clearly indicates that the ladders do not contain a significant systematic error (i.e.,  $T_{eff}$  is appropriate).

**Lithium Binding Energies.** In Table 3, the lithium ion binding energies of the *N*-acetyl and *N*-glycyl amino acids are listed. In general, the lithium binding energies display the same patterns that were seen in the proton affinities; the amino acid derivatives with basic side chains have the highest binding energies, and the amino acid derivatives with alkyl side chains (Gly, Ala) have low binding energies. However, there are some notable differences between the proton and lithium ion binding energies. In particular, the presence of an oxygen in the side chain greatly enhances the lithium binding energy. For example, the gas-phase basicity of glycyserine (GS) is about 1 kcal/mol less than the gas phase basicity of glycyvaline (GV), but the lithium binding energy of GS is 3 kcal/mol higher than that of GV. The effect of amino acids with coordinating atoms in the side chain can clearly be seen in a plot (Figure 2a) of  $\Delta\Delta G_{Li}$  vs  $\Delta GB$  for the *N*-glycyl derivatives (throughout the discussion, the additional  $\Delta$  refers to values relative to the anchor compounds). For the 14 derivatives, the plot shows a good deal of scatter, indicating that there is no direct correlation between  $Li^+$  and  $H^+$  binding energies. In other words, lithium cations exhibit binding preferences that are significantly different than those for protons. However, if one limits the analysis to the amino acids with alkyl side chains (i.e., Gly, Ala, Val, Leu, Pro), a good correlation can be found. These points are shaded in the graph, and the correlation line is also shown in Figure 2a. Several points are far above the line (Ser, Asp, Thr, Glu, and Trp) and therefore exhibit unusually high lithium binding energies (as compared to gas-phase basicities). Each of these derivatives contains an oxygen or nitrogen atom in the side chain, and therefore, multidentate coordination involving the side chain is a possibility. In fact, all of the derivatives with

(51) The amine references were *sec*-butylamine, *N*-ethylmethylamine, trimethylamine, *N,N*-dimethylethylamine, and *N,N*-diethylmethylamine. The following GB values were used: 214.1, 217.3, 219.4, 222.1, 224.7 kcal/mol, respectively. They are from the Hunter and Lias compilation.

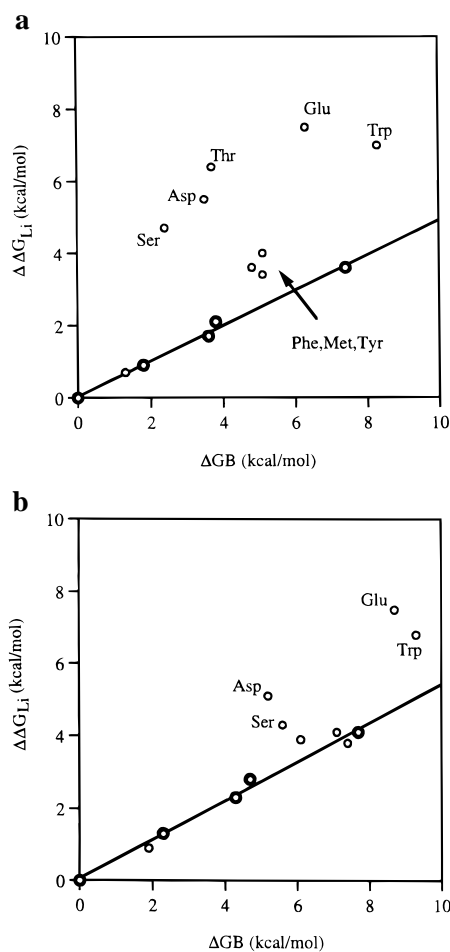


**Figure 2.** (a) Plot of the relative lithium ion binding energies ( $\Delta\Delta G_{Li}$ ) of the glycylylated amino acids vs their relative gas-phase basicities ( $\Delta GB$ ). (b) Plot of the relative lithium ion binding energies ( $\Delta\Delta G_{Li}$ ) of the acetylated amino acids vs their relative gas-phase basicities ( $\Delta GB$ ). In each case, the correlation line is a least-squares fit to the amino acids with alkyl side chains (Gly, Ala, Val, Leu, and Pro). These points are represented with heavy circles.

coordinating side chains have unusually high lithium binding energies with the exception of tyrosine, but the orientation of the phenol oxygen makes multidentate chelation unlikely for glycytyrosine. Although the protonated species could engage in similar behavior (i.e., hydrogen bonding to the side chain), the larger size of the lithium cation probably facilitates the multidentate coordination and leads to the enhanced binding energies. The Phe, Met, and Tyr derivatives are also slightly above the line. The deviation is much less significant, but lithium is known to have a reasonably high affinity for aryl groups (this does not explain Met).<sup>19–21</sup>

The interaction of the side chain with the lithium was explored with molecular dynamics. Using glycyserine as a model, simulations (CHARMm) indicate that the lithium is generally located at the amide carbonyl. This is in contrast to protonated glycyserine where the charge carrier resides on the *N*-amino group. With the lithium coordinated to the amide carbonyl, favorable interactions are possible with the serine hydroxyl group. Many low-energy conformations exhibit this interaction, and minimization of low-energy conformers from the simulation suggests that the global minimum has the lithium coordinated to the two carbonyls (amide and C-terminal carboxyl) as well as the serine hydroxyl. In addition, the average structures from the simulations display a fairly short distance between the lithium and the hydroxyl oxygen. For example, a simulation at

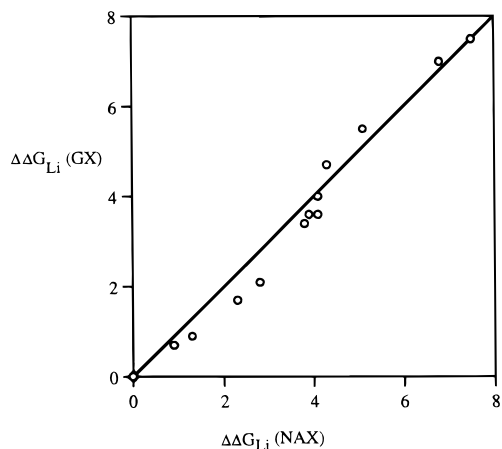


**Figure 3.** Plot of the relative lithium binding energies of the glycyated amino acids (GX) vs the acetylated amino acids (NAX). Values in kcal/mol. A 1:1 correlation line (slope = 1, intercept = 0) is superimposed on the plot.

350 K (250 ps)<sup>52</sup> gives average oxygen/lithium distances of 1.92, 1.88, and 1.85 Å for the serine hydroxyl, amide carbonyl, and carboxyl carbonyl, respectively.<sup>53</sup> Simulations with glycyglutamic acid lead to similar conclusions. These results provide a rational explanation for the data presented in Figure 2a. Because side-chain coordination appears to be important in the lithiated, but not the protonated *N*-glycyl derivatives, it is not surprising that substrates containing residues such as serine and glutamic acid would exhibit enhanced lithium affinities (relative to their proton affinities).

The *N*-acetyl amino acids give the same pattern in a plot of  $\Delta\Delta G_{\text{Li}}$  vs  $\Delta\text{GB}$  (Figure 2b). Again, the derivatives with coordination sites in the side chain are above the correlation line and exhibit unusually high lithium binding energies; however, the differences are not as dramatic. This is not a result of changes in the lithium binding. For example, glycyserine and acetylserine have nearly the same  $\Delta\Delta G_{\text{Li}}$  values (4.7 vs 4.3 kcal/mol). As noted above, the GBs of the acetylated derivatives are more sensitive to coordinating groups in the side chain because protonation of the amide places the charge site in a satisfactory location for hydrogen bonding to the side-chain functional group. As a result, the  $\Delta\text{GB}$  values for Ser, Glu, Asp, and Trp are significantly higher in the acetylated series (as compared to the glycyated series) and the benefit of lithium binding to coordinating side chains appears to be attenuated (i.e. the points for these derivatives are shifted to the right in Figure 2b). In other words, some of the energetic advantage of side-chain coordination is already manifested in the protonated acetyl derivatives.

Recently there has been much speculation about the metalation of zwitterionic forms of peptides in the gas phase.<sup>54–57</sup>

(52) During the entire 250-ps simulation at 350 K, the complex retained the tricoordinate structure.

(53) At higher temperatures, the average distance between the serine and the hydroxyl oxygen increases because entropy disfavors the highly ordered, tricoordinate structure. As a result, the interaction with the serine hydroxyl is absent in the majority of the structures. For example, a simulation at 800 K (250 ps) yielded an average lithium/serine hydroxyl distance of 4.84 Å; however, the average lithium/carbonyl oxygen distances remained short (<2 Å). This result highlights the fact that subtle binding interactions can be obscured when metal/ligand complexes are studied at high temperatures.

(54) Price, W. D.; Jockusch, R. A.; Williams, E. R. *J. Am. Chem. Soc.* **1997**, *119*, 11988.

(55) Campbell, S.; Rodgers, M. T.; Marzluff, E. M.; Beauchamp, J. L. *J. Am. Chem. Soc.* **1995**, *117*, 12840.

(56) Lee, S.-W.; Kim, H. S.; Beauchamp, J. L. *J. Am. Chem. Soc.* **1988**, *120*, 3188.

**Table 4.** Sodium Binding Energies of Dipeptides

X	$\Delta G_{\text{Na}}$ (kcal/mol)	
	<i>N</i> -Gly-X	<i>N</i> -acetyl-X
Trp	41.2	37.4
Pro	38.9	35.2
Glu	40.7	37.0
Tyr	38.0	34.6
Met	37.4	34.3
Phe	38.1	34.8
Leu	36.9	33.9
Thr	38.6	<i>a</i>
Val	36.7	33.5
Asp	38.5	34.9
Ser	37.4	33.9
Ala	35.5	32.1
Cys	34.3	30.9
Gly	34.2	30.8

<sup>a</sup> *N*-acetyl threonine was not included in the study.

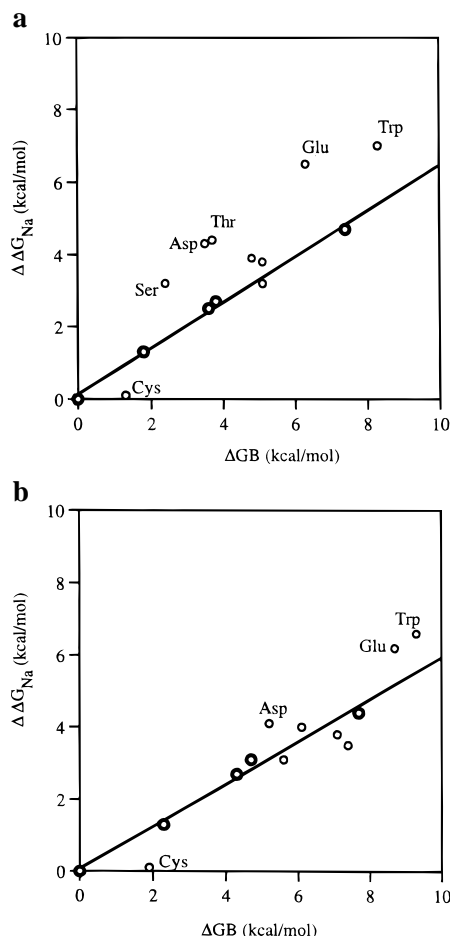


**Figure 4.** (a) Plot of the relative sodium ion binding energies ( $\Delta\Delta G_{\text{Na}}$ ) of the glycyated amino acids vs their relative gas-phase basicities ( $\Delta\text{GB}$ ). (b) Plot of the relative sodium ion binding energies ( $\Delta\Delta G_{\text{Na}}$ ) of the acetylated amino acids vs their relative gas-phase basicities ( $\Delta\text{GB}$ ). In each case, the correlation line is a least-squares fit to the amino acids with alkyl side chains (Gly, Ala, Val, Leu, and Pro). These points are represented with heavy circles.

Our data provides insight into this issue because zwitterion formation is possible for the glycy derivatives, but highly unlikely for the acetyl derivatives (no *N*-terminal amino group). A plot comparing  $\Delta\Delta G_{\text{Li}}$  for the two series is given in Figure 3. A 1:1 correlation line (intercept = 0) has been applied to the

(57) Schnier, P. D.; Price, W. D.; Jockusch, R. A.; Williams, E. R. *J. Am. Chem. Soc.* **1996**, *118*, 7178.

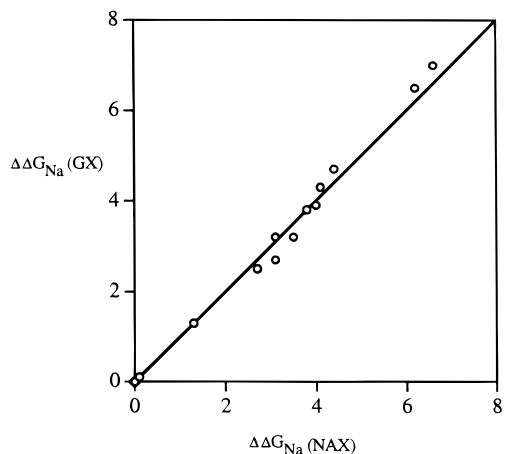


**Figure 5.** Plot of the relative sodium binding energies of the glycylation (GX) vs the acetylation (NAX). Values in kcal/mol. A 1:1 correlation line (slope = 1, intercept = 0) is superimposed on the plot.

plot. It can be seen that none of the points deviates from this line by more than  $\sim 0.2$  kcal/mol so that the side chains are having almost identical effects on the lithium binding of the acetylated and glycylation systems. This strongly suggests that the ESI generated ions are not adopting zwitterionic structures. If the glycylation series were zwitterionic, one would expect some derivatives to have unusually high or low affinities due to the radically different coordination scheme. In contrast, the good correlation between the two series of compounds indicates that they probably adopt similar coordination schemes.

**Sodium Ion Binding Energies.** The sodium ion binding energies of the *N*-glycyl and *N*-acetyl amino acids are listed in Table 4. Similar patterns are observed in the plots of  $\Delta\Delta G_{\text{Na}}$  vs  $\Delta\text{GB}$  for the sodium series (Figure 4). The amino acid derivatives with alkyl side chains give a good correlation line, but several of the derivatives with coordinating side chains lie above this line. As with the lithium complexes, glycylation Glu, Asp, Ser, Trp, and Thr exhibit unusually high ion binding energies (Figure 4a). The effect is not as pronounced as with lithium, partly because sodium ion binding energies are naturally lower than lithium ion binding energies. The sodium complexes of the acetylation amino acids also mirror the pattern seen with lithium. The Asp, Glu, and Trp derivatives lie above the correlation line, but the deviation is less than with the glycylation

systems (Figure 4b). As noted above, the reason for the reduced effect is that GB is more sensitive to the nature of the side chain when the *N*-terminal amino group is missing and the points for the coordinating side chains are all shifted to the right. One significant difference is that acetylation serine is slightly below the correlation line for the sodium complex. This is a direct result of the high  $\Delta\text{GB}$  of acetylation serine, not an unusually low  $\Delta\Delta G_{\text{Na}}$ . The  $\Delta\Delta G_{\text{Na}}$  of acetylation serine is approximately the same as that of glycylation serine (3.1 vs 3.2 kcal/mol). A plot comparing the two series (Figure 5) again indicates that the side chains have the same effect on the acetylation and glycylation systems. The small deviations from the 1:1 correlation line strongly suggest that both series adopt the same coordination scheme (i.e., zwitterions are not important).

In Figure 4a and b, the points for *N*-acetyl and *N*-glycyl cysteine fall below the correlation line defined by the amino acids with alkyl side chains. In fact, the sodium ion binding energies of the cysteine derivatives are almost identical to those of the glycine derivatives. In other words, the  $-\text{CH}_2\text{SH}$  group provides virtually no stabilization to the sodiated system. A logical explanation is that the presence of the  $\text{CH}_2\text{SH}$  group limits (sterically hinders) the peptide's ability to adopt a favorable conformation for multidentate chelation to the sodium.

## Conclusions

The lithium and sodium binding energies of a series of acetylation and glycylation amino acids indicates that multidentate chelation plays an important role in the binding. In particular, the amino acids with coordinating groups in the side chain exhibit enhanced metal ion binding energies. The gas-phase basicities of the peptide derivatives indicate that hydrogen bonding to Lewis bases in the amino acid side chain is more important for the acetylation amino acids than for the glycylation amino acids. The metal ion binding energies of the acetylation and glycylation amino acids exhibit very similar patterns. This result suggests that they adopt similar coordination schemes and that it is unlikely that zwitterionic forms of the peptides are involved.

**Acknowledgment.** Support from the National Center for Research Resources (Research Infrastructure in Minority Institutions P20 RR11805) of the National Institutes of Health is gratefully acknowledged.

JA983116S